

INSTRUMENTS AND METHODS OF INVESTIGATION

PACS numbers: **42.79.–e**, **44.10.+i**

Large-sized mirrors for power optics

V Yu Khomich, V A Shmakov

DOI: https://doi.org/10.3367/UFNe.2018.10.038465

Contents

Abstract. **Research on the fabrication of large-sized mirrors for power optics from such materials as invar, SiC, and the C–Si–SiC composite material are discussed. Methods to calculate thermal deformations in cooled mirrors under irradiation with light have been developed. A technique to reduce the mirror weight is suggested that is based on employing materials consisting of multilayered cellular structures and porous materials.**

Keywords: materials for mirrors, heat transfer, thermal deformation, mirror stability parameters

1. Introduction

The question of developing the large-sized laser mirror attracts more attention every year. This is connected with the need to fabricate new laser complexes for various applications, which include:

— special technologies under some production conditions (cutting of materials and metal construction, welding and case-hardening);

— shoreline and water surface treatment after accidental oil spills, including removal of rainbow oil films, which can not be efficiently destroyed applying other methods;

— contactless cutting of metal and reinforced concrete construction during disassembly and emergency maintenance at oil and gas wells and nuclear power plants, as well as during the cutting of ship hulls for scrap metal and rescue operations in the case of natural disasters and terrorist attacks;

— processing of metallurgical, chemical, and mining equipment during maintenance and assembly, as well as in specialized equipment applications.

Laser mirrors can undergo various types of mechanical and thermal loads, depending on their operating conditions. Even small absorption of incident light may cause thermal deformations, which ultimately lead to significant changes in the optical surface shape and corresponding distortions of the wave front of the generated radiation. This means that one needs to carefully select the mirror material and solve the problem of its thermal regulation — that is, developing an efficient mirror cooling system.

This paper clearly demonstrates that the thermal stability of cooled mirrors significantly depends on heat conduction, the thermal expansion coefficient, and the heat-sink capacity of the mirror material, which are the main factors that define optical performance capabilities. We study the feasibility of creating cooled large-sized mirrors from such materials as invar, silicon carbide, and carbon–silicon–silicon carbide composite. A method for large-sized mirror mass reduction is suggested based on the utilization of multilayered cellular and porous structures, which greatly decreases the weight of the mirror and the time of its thermal stabilization.

2. Calculation of thermal deformations in laser mirrors

Calculations of thermal deformations in large-sized mirrors are concerned with solving the spatial problem of thermoelasticity for a finite body. Known solutions for semiinfinite bodies are incorrect in this case, because the boundary conditions on side surfaces play a significant role. This task can be solved in reality by choosing an appropriate model which would take into account the main factors influencing the development of thermal deformations in mirrors. In this paper, we choose the model of a thick plate.

Let us consider a mirror to be a multilayered plate consisting of various isotropic materials. Such a mirror is schematically drawn in Fig. 1. For clarity, we have chosen a rectangular shape. The reflective plate, heat exchanger, and heavy-duty frame of the mirror shown in the figure can be considered a three-layer plate. We assume that the layers are

V Yu Khomich [(1)], **V A Shmakov** [(2)]
[(1)] Institute for Electrophysics and Electric Power, Russian Academy of Sciences, Dvortsovaya nab. 18, 191186 St. Petersburg, Russian Federation
[(2)] Prokhorov General Physics Institute, Russian Academy of Sciences, ul. Vavilova 38, 119991 Moscow, Russian Federation
E-mail: [(1)] Khomich@ras.ru, [(2)] shmakov@kapella.gpi.ru

Received 18 January 2018
Uspekhi Fizicheskikh Nauk **189** (3) 263 – 270 (2019)
DOI: https://doi.org/10.3367/UFNr.2018.10.038465
Translated by A L Chekhov; edited by A Radzig

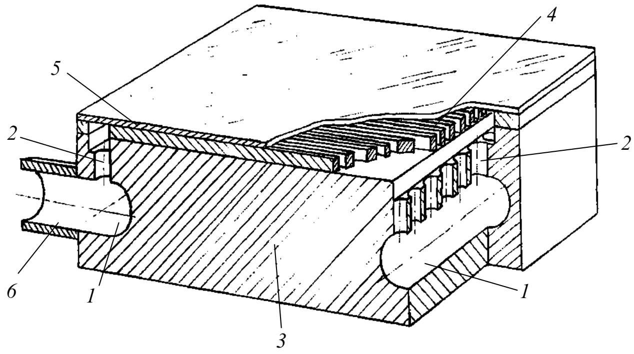

Figure 1. Cooled laser mirror: *1* and *2* — collector system for supply and removal of the heat transfer agent, *3* — heavy-duty frame of the mirror, *4* — channel type heat exchanger with slit-like channels, *5* — reflective plate, and *6* — barb fitting.

tightly attached to each other along the interfaces, so there is no sliding between them during development of deformations, and the multilayered plate acts as a whole.

When calculating thermoelastic deformations within the proposed model, the bending deformation is accompanied by a thermal expansion deformation normal to the neutral surface. This model allows taking into account the inhomogeneous structure of the mirror in different layers and analyzing results for different combinations of materials. The interaction between the layers is included, using the reduced coefficient of the transverse contraction $\tilde{\nu}$ (reduced Poisson ratio), which is defined by the geometry and materials of the layers.

Between the boundary surfaces of the multilayered plate there is a neutral surface, which does not deform under pure bending. We accept the Kirchhoff–Love hypotheses, which state that the elements normal to the neutral surface (straight fibers of the plate) remain straight and normal to the deformed neutral surface without changing their length. We also assume that the normal stresses on the planes parallel to the neutral surface of the plate can be ignored, because they are small with respect to other stresses. Moreover, the temperature field is assumed not to cause significant bending strains in the neutral surface of the plate (the stretching influence on the neutral surface bending is ignored).

Displacements of the mirror's reflective surface under a thermal load can be defined in the present model as the sum of bending displacements W_{bend} and thermal expansion W_{exp} normal to the neutral surface:

$$W = W_{\text{bend}} + W_{\text{exp}} .$$

Displacements corresponding to inhomogeneous thermal expansion W_{exp} can be expressed as the difference between the displacements of the optical and neutral surfaces:

$$W_{\text{exp}} = \int_0^{z_0} T(z)\,\beta(z)\,\mathrm{d}z ,$$

where $\beta(z)$ is the linear expansion coefficient, and z_0 is the distance between the reflective and neutral surfaces, which can be found from the condition

$$\int_{z_0-H}^{z_0} Ez\,\mathrm{d}z = 0 .$$

Here, H is the mirror thickness, and E is the Young's modulus.

The value of the bending contribution to the optical surface displacement can be found from solving the bending equation

$$\nabla^4 W_{\text{bend}} = -\nabla^2 M_T D , \tag{1}$$

where M_T is the temperature moment:

$$M_T = \int_{z_0-H}^{z_0} \frac{E\beta z}{1-\tilde{\nu}}\, T(r,t)\,\mathrm{d}z ,$$

D is the reduced plate bending stiffness:

$$D = \int_{z_0-H}^{z_0} \frac{E(\tilde{\nu}-\nu)}{1-\tilde{\nu}^2}\,\mathrm{d}z ,$$

while the reduced Poisson ratio $\tilde{\nu}$ can be obtained from the condition

$$\int_{z_0-H}^{z_0} \frac{E(\tilde{\nu}-\nu)}{1-\tilde{\nu}^2}\,\mathrm{d}z = 0 .$$

For an axially symmetric problem, the boundary conditions of a freely supported round plate with radius R will have the following form:

$$\begin{cases} W_{\text{bend}}(r) = 0 , \\ \nabla^2 W_{\text{bend}}(r) + \dfrac{\nu-1}{r}\,\dfrac{\mathrm{d}W_{\text{bend}}(r)}{\mathrm{d}r} = -\dfrac{M_T}{D} \end{cases} \quad \text{for} \quad r = R . \tag{2}$$

Equation (1) and boundary conditions (2) do not contain inertial terms, which means that we consider the problem of thermoelastic displacements of an optical surface in the quasi-stationary approximation. This approximation assumes that deformations and stresses reach steady-state values much faster than the temperature; therefore, the nonstationarity is taken into account only in the heat conduction equation.

We will search for the solution of equation (1) in the form

$$W_{\text{bend}} = C_1(r^2 - R^2) + \sum_{k=1}^{\infty} W_k \frac{J_0(\beta_k r/R)\sqrt{2}}{RJ_1(\beta_k)} , \tag{3}$$

where J_0 and J_1 are, respectively, zero- and first-order Bessel functions of the first kind, and β_k are the solutions of the equation $J_0(\beta_k) = 0$. The first term in formula (3) is the solution of equation (1) for a thermal flux constant along the radius, while the second term takes into account the inhomogeneity of this flux.

Let us now expand the temperature load M_T/D into a series:

$$\frac{M_T}{D} = \sum_{m=0}^{\infty} \theta_{\text{m}} \frac{J_0(\alpha_m r/R)\sqrt{2}}{RJ_0(\alpha_m)} . \tag{4}$$

Here, α_m are the solutions of the equation $J_1(\alpha_m) = 0$.

Taking into account that

$$\nabla^2 J_0\left(\frac{\beta_k r}{R}\right) = -\left(\frac{\beta_k}{R}\right)^2 J_0\left(\frac{\beta_k r}{R}\right) ,$$

we obtain the relationship

$$\nabla^4 W_{\text{bend}} = \sum_{k=1}^{\infty} W_k \frac{J_0(\beta_k r/R)\sqrt{2}}{RJ_1(\beta_k)} \left(\frac{\beta_k}{R}\right)^4 . \tag{5}$$

Table 1. Temperature and displacements of an optical surface for a cooled copper mirror.

Interlayer boundary coordinate	$t = 0.01$ s	$t = 0.55$ s	$t = 1.9$ s	$t = 3.73$ s	$t = 6.2$ s	$t = 28$ s
0 (optical surface)	0.31	1.68	1.85	1.93	1.97	2.07
1 mm (below the reflecting plate)	0.11	1.30	1.46	1.54	1.57	1.68
3.5 mm (below the heat exchanger)	0.001	0.43	0.62	0.71	0.76	0.89
65 mm (rear side)	0	0	0	0.01	0.06	0.42
Optical surface displacements, μm	0.04	0.71	1.19	1.43	1.51	1.26

Let us expand the function $J_0(\alpha_m r/R)$ into a Fourier series as well:

$$J_0\left(\frac{\alpha_m r}{R}\right) = \sum_{k=1}^{\infty} C_k \, \frac{J_0(\beta_k r/R)\sqrt{2}}{RJ_1(\beta_k)} = \sum_{k=1}^{\infty} \frac{2J_0(\beta_k r/R)}{J_1(\beta_k)(\beta_k^2 - \alpha_m^2)}\, \beta_k J_0(\alpha_m)\,,$$

$$C_k = \int_0^R J_0\left(\frac{\alpha_m r}{R}\right) r J_0\left(\frac{\beta_k r}{R}\right) \mathrm{d}r = \frac{R\beta_k}{\alpha_m^2 - \beta_k^2}\, J_0(\alpha_m)\, J_1(\beta_k)\,.$$

The temperature load (4) can now be expressed in the form

$$\frac{M_T}{D} = \sum_{m=0}^{\infty}\sum_{k=1}^{\infty} \theta_{\mathrm{m}} \, \frac{2\sqrt{2}J_0(\beta_k r/R)\,\beta_k J_0(\alpha_m)}{RJ_0(\alpha_m)\,J_1(\beta_k)(\beta_k^2 - \alpha_m^2)} = \sum_{m=0}^{\infty}\sum_{k=1}^{\infty} \chi_{mk}\, \frac{\sqrt{2}J_0(\beta_k r/R)}{RJ_1(\beta_k)}\,. \tag{6}$$

Here, we introduced a factor $\chi_{mk} = \theta_{\mathrm{m}} 2\beta_k/(\beta_k^2 - \alpha_m^2)$. Using formula (6), we arrive at

$$-\nabla_r^2 \frac{M_T}{D} = \sum_{k=1}^{\infty}\sum_{m=0}^{\infty} \chi_{mk}\, \frac{\sqrt{2}J_0(\beta_k r/R)}{RJ_1(\beta_k)} \left(\frac{\beta_k}{R}\right)^2, \tag{7}$$

and by comparing formulas (5) and (7), we derive

$$W_k = \sum_{m=0}^{\infty} \frac{\chi_{mk}}{(\beta_k/R)^2}\,. \tag{8}$$

Now, taking into account Eqn (8) and boundary conditions (2), it is fashionable to define the constant C_1 in equation (3):

$$C_1 = \frac{v-1}{2(1+v)} \sum_{k=1}^{\infty}\sum_{m=0}^{\infty} \chi_{mk}\, \frac{\sqrt{2}}{R\beta_k}\,.$$

Finally, we obtain for W_{bend} the following expression

$$W_{\mathrm{bend}} = \frac{v-1}{2(1+v)} \sum_{k=1}^{\infty}\sum_{m=0}^{\infty} \chi_{mk}\, \frac{\sqrt{2}(r^2 - R^2)}{R\beta_k} + \sum_{k=1}^{\infty}\sum_{m=0}^{\infty} \frac{\chi_{mk}}{(\beta_k/R)^2}\, \frac{\sqrt{2}J_0(\beta_k r/R)}{RJ_1(\beta_k)}\,. \tag{9}$$

This means that for a given temperature distribution inside the mirror one can obtain the displacement of the reflecting surface with respect to the initial position. In a real cooled mirror, the dimensions of the cooling region (usually with high temperature gradients) are small with respect to the total dimensions of the mirror. It is very hard to solve the problem of calculating the temperature fields with boundary conditions given for the whole mirror surface, including the wetting surfaces of the cooling channels.

As in the case of thermal deformation, calculating the temperature field can be done by using the multilayered plate model of a cooled mirror. In this case, one or several layers are replaced by a homogeneous medium with reduced thermophysical characteristics, while the heat exchangers are considered heat sinks with distributed bulk heat-transfer coefficients. Such a model allows taking into account the inhomogeneity of the mirror structure and reaching satisfactory agreement between the temperature field calculated results and the experimental data. The method for temperature field calculations in the given system is presented in book [1].

Table 1 lists the temperatures and displacements of the optical surface of a cooled copper mirror with a diameter of 350 mm for a constant heat flux of 10 W cm^{-2} on the optical surface. The thickness of the mirror is $H = 65$ mm, the thickness of the reflecting plate is $h = 1$ mm, the thickness of the cooling layer is 2.5 mm, the width of the channel inside the heat exchanger is $l = 0.6$ mm, the edge thickness is $\delta = 0.9$ mm, the heat-transfer coefficient is set to $\alpha = 1.5$ W cm^{-2} deg^{-1}, and the heat conduction $\lambda_r = \lambda_z = 1.3$ W sm^{-2} deg^{-1}.

As the calculated results show, the setting time of the stationary operation regime for such a mirror can be large (in this case, it lasts approximately 30 s). In order to reach the stationary regime faster (decrease the mirror temperature stabilization time), one will need to utilize highly nonconventional designs. Besides the known heat exchangers, such mirrors should also have a thermal stabilization system for the heavy-duty frame. This is also relevant to other types of thermal action (change in the temperature of the surroundings, influence of the Sun or wind, etc.).

3. Thermal stability parameters of laser mirrors

Thermal stability parameters of laser mirrors were introduced for the pulsed-periodic operating regime in the pioneering studies on power optics [2, 3].

One of the most important requirements for large-sized mirror materials is the constancy of their optical characteristics. Monitored parameters usually include the reflection coefficient, complex refractive index, thermal expansion coefficient, density, heat conduction, specific heat capacity, and melting point [4].

No less important characteristics also include:

• mechanical — modulus of elasticity, tensile strength, yield stress, microhardness;

• metallographic — crystal structure, grain size, recrystallization temperature, stress-relief temperature, existence of a second phase, pores and impurities;

• technological — these factors define the potential to perform mechanical processing, polishing, and the application of coatings.

Common disadvantages of the mirrors conventionally used in large-sized optics made of copper, glass-ceramics, fused quartz, sitall, and other materials are the high thermal expansion coefficient or low heat conduction. Such mirrors cannot be efficiently used for high-intensity luminous fluxes and under fast variations of the ambient temperature.

The thermal stability of the mirrors with respect to the luminous load is defined by a number of parameters. Based on the criterion of the reflecting surface reaching the critical temperature, the stability parameters for continuous and pulsed operation regimes have, respectively, the following form

$$\max\{\lambda T\}, \quad \max\{\sqrt{\lambda c \rho}\, T_{\mathrm{cr}}\},$$

where c is the specific heat capacity, λ the heat conduction coefficient, and ρ the density of the material. Critical temperature T_{cr} has its own physical meaning for a specific material: melting point, origin of the recrystallization process, phase transitions, etc. Here and further, 'max' denotes the maximal acceptable value of the specified parameter for the specified material, for which the optical performance of the mirror remains constant.

Part of radiation absorbed by the optical surface is transferred into heat and creates heat fluxes inside the material. This leads to the formation of an inhomogeneous temperature distribution inside the mirror and causes thermal stresses. If the heat flux induced maximal tangential stresses exceeding the material microyield strength, irreversible structural changes take place. Corresponding material stability parameters with respect to the appearance of plastic deformations on the optical surface have the following form for the mentioned laser operation regimes:

$$\max\left\{\frac{\lambda\sigma_0}{\beta E}\right\}, \quad \max\left\{\frac{\sqrt{\lambda c\rho}\,\sigma_0}{\beta E}\right\},$$

where σ_0 is the microyield strength, β the thermal expansion coefficient, and E the Young's modulus. Quantities σ_0 and E should be considered simultaneously, because the high level of temperature stresses ($\approx \beta E/\lambda$) may not lead to the appearance of structural changes in the material, if the microyield strength is high enough. For fragile materials, as the value of σ_0 one should use the fragile breaking stress or the origin of microcrack formation. Plastic materials are characterized by the residual deformation level, which leads to a worsening of the optical properties of the reflecting surface. Ultimate stress σ_0, which is defined in this case experimentally, corresponds to the value of $\sigma_{0.01}$ — stress that causes 0.01 deformation. For pulsed-periodic laser operation, one needs to take into account the fatigue damage of the material.

Thermoelastic distortion of the mirror reflecting surface is one of the main characteristics which gives a considerable estimate for the laser radiation quality. Material stability parameters related to the values of ultimate distortion of the optical surface for continuous and pulsed laser operations, namely

$$\max\left\{\frac{\beta}{\lambda}\right\}, \quad \max\left\{\frac{\beta}{c\rho}\right\},$$

can be obtained based on the solution to model problems of thermoelasticity.

For each operation regime there is the 'stiffest' stability parameter, which limits the choice of the materials for laser mirrors. For a continuous operation regime, 'stiff' parameters include the parameter describing thermoelastic deformation of the optical surface and the parameter responsible for the appearance of plastic deformations. For pulsed lasers, these parameters correspond to the optical surface reaching the critical temperature and the conditions for plasma formation. As the pulse length decreases, the parameters that describe the melting of the material, evaporation, and appearance of surface plasma become greater in importance. If the pulse length is $\approx 10^{-9}$ s or less, the dynamical effects become important. In this case, one should take into consideration the finiteness of the heat transfer rate and of the elastic wave velocities.

Some of the requirements for cooled mirrors can be mutually exclusive. Let us consider, for example, the thermal stability parameters defined by the ultimate heat flux and ultimate thermal distortion of the optical surface. The reduction in mirror thermal deformations by design optimization is connected to the appearance of additional stresses that prevent optical surface distortion. This leads to the lowering of the ultimate heat fluxes, at which the plastic deformation of the optical surface originates. Moreover, increasing cooling system efficiency by decreasing the sizes of the heat-exchanger single elements can lead to a drop in the laser mirror rigidity.

The choice of stability parameters for continuous laser mirrors with an advanced cooling system is related to the thermal exchange features, which can significantly change the deformation properties. The temperature field of the cooled laser mirror is usually concentrated in a thin layer adjacent to the reflecting surface. Heat exchange proceeds through heat transfer, while the heat conduction coefficient is of less importance than for uncooled mirrors.

Figure 2 plots the dependence of optical surface distortions on the heat conduction, $W = W(\lambda)$, calculated for a cooled mirror with a characteristic size of 500 mm and $\beta = 1.7 \times 10^{-7}$ K^{-1}(copper). As one can see from the figure, this dependence strongly deviates from the known law

$$W \approx \frac{\beta}{\lambda}.$$

For heat conductions above 100 W m^{-1} K^{-1} the distortion W varies weakly. For example, if λ is increased from 100 to 400 W m^{-1} K^{-1}, the value of W decreases by only 27%, which means that for this region the choice of the

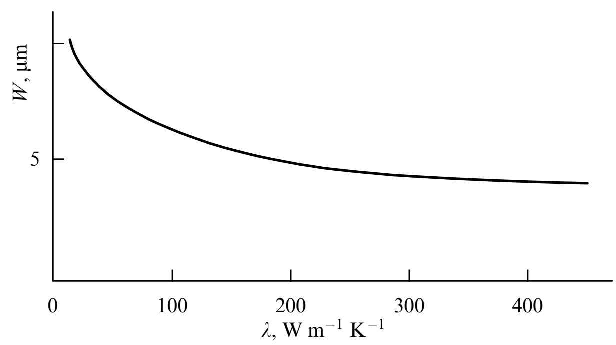

Figure. 2. Thermal displacements of the reflecting surface versus the mirror material heat conduction.

material for laser mirrors strongly depends on the thermal expansion coefficient. As further analysis will demonstrate, the choice of heat-transfer agent plays an important role in this case as well.

To clarify this dependence, let us consider the following problem. We will suppose that the laser mirror consists of a thin reflecting plate with thickness h and a massive base with a heat exchanger between them. The thermophysical characteristics of the heat exchanger are defined by the heat conduction coefficient λ_Π, bulk heat-transfer coefficient α_v, and porosity Π. We will also assume that the heat is concentrated inside the reflecting plate and the adjacent area of the heat exchanger. The mirror base remains thermally insulated.

Distortions of the optical surface are in this case caused by the thermal expansion of the reflecting plate with a linear distribution of temperature and by the heated adjacent area of the heat exchanger with an exponential temperature distribution. With all the above considerations taken into account, such a distortion may be expressed as

$$W_\mathrm{norm} \approx \beta \left(\frac{1}{\alpha_\mathrm{v}} + \frac{h}{\sqrt{\alpha_\mathrm{v} \lambda_\Pi}} + \frac{h^2}{2\lambda} \right).$$

The first term in the obtained expression corresponds to the deformation of the cooling layer, while the second and the third ones to the reflecting plate expansion.

Using the analytical solution for bending, one can show that the deformations take the form

$$W_\mathrm{bend} \approx \beta \, \frac{h}{\sqrt{\alpha_\mathrm{v} \lambda_\Pi}} .$$

Total distortion of the optical surface is

$$W = W_\mathrm{norm} + W_\mathrm{bend} .$$

Let us introduce a dimensionless parameter

$$k = \frac{h}{2} \sqrt{\frac{\alpha_\mathrm{v}}{\lambda_\Pi}} .$$

Heat conduction coefficient λ_Π of the heat exchanger medium may be expressed through the porosity and heat conduction coefficient of the initial material:

$$\lambda_\Pi = \lambda(1 - \Pi) .$$

Then, one obtains

$$W \approx \frac{\beta}{\alpha_\mathrm{v}} \left[1 + 4k + 2k^2(1 - \Pi) \right] . \tag{10}$$

Heat conduction coefficient is indirectly enters expression (10) through the k parameter. The bulk heat-transfer coefficient takes into account the properties of the heat-transfer agent and the peculiarities of the heat exchanger design. This means that the stability parameter of the cooled mirrors depends not only on the heat conduction and thermal expansion coefficients of their material. Details of the mirror design and the heat-transfer agent play an important role as well.

It follows from expression (10) that by turning the thickness of the reflecting plate to zero one may achieve the result: the stability parameter becomes independent of the material heat conduction and is only defined by the ratio of the coefficient of thermal expansion to the bulk heat-transfer coefficient:

$$W \approx \frac{\beta}{\alpha_\mathrm{v}} .$$

For large k, the parameter becomes proportional to β/λ, which brings us to a well-known relation.

Table 2 collates several materials which have been suggested for mirror fabrication. Luminous flux density and mirror design are chosen to be such that the distortion W of the optical surface would be close to 1 μm for copper mirrors with a channel cooling system (see Fig. 1). Moreover, Table 2 also shows the deflection E/ρ of the optical surface under its own weight, the maximal temperature ΔT_max on the reflecting surface for the luminous load and mirror design mentioned above, as well as the luminous flux density $\sigma_T/(E\beta\Delta T_\mathrm{max})$ (σ_T is the yield stress of the mirror material) on the reflecting surface, which may lead to developing plastic deformations of the mirror material.

As one can see from Table 2, thermoelastic deformations ε_T of the optical surface of mirrors made of tungsten and molybdenum are ≈ 0.4 times that for copper mirrors. Moreover, due to high yield stress, tungsten can withstand higher thermal flux densities than molybdenum and copper.

Table 2. Characteristics of materials suggested for mirror fabrication.

Material	λ, W m^{-1} K^{-1}	$\beta \times 10^6$, K^{-1}	$E \times 10^{-10}$, N m^{-2}	$\sigma \times 10^{-7}$, N m^{-2}	$\rho \times 10^{-3}$, kg m^{-3}	ε_T, μm	$(E/\rho) \times 10^{-2}$	ΔT_max	$\sigma/(E\beta\Delta T_\mathrm{max})$
Strained copper	400	17.4	11.2	6.85	8.93	1.02	1.25	12.5	2.8
Tungsten	160	4.5	40	10.8	19.1	0.36	2.1	22.2	9.3
Molybdenum	130	5.2	31	29.4	9.01	0.40	3.4	19.7	2.7
Stainless steel	20	16.6	20.0	23.5	7.85	1.9	2.55	79.9	0.87
Nickel	92	13.3	20.2	20.5	8.90	1.13	2.27	26.0	2.9
Aluminum	211	24.5	6.85	6.44	2.70	1.77	2.54	17.2	22
Titanium	15.5	8.5	10.9	7.5	4.54	1.06	2.42	101	0.8
Beryllium	182	13.7	33	—	1.85	1.03	17.8	18.4	—
Invar	11	1.6	14.7	—	8.00	0.22	1.84	145	8.00
Silicon	140	3.0	11.3	—	2.42	0.24	4.67	21.5	—
Silicon carbide	110	3.3	39.2	—	3.2	0.28	12.2	25	—

For large-sized laser mirrors located in the large-aperture beam lines, the densities of the luminous load are not high (for a constant integral power of a laser beam), while the temperature of the reflecting surface is lower than in mirrors under a high load. This allows using invar as the material for large-sized mirrors. This material retains its physicomechanical characteristics only at temperatures close to room temperature. Silicon carbide and composite materials based on it can be used in this case as well.

4. Problem of weight reduction for large-sized mirrors

We will model the whole construction of a large-sized mirror as a round and relatively thick plate, which is freely supported along the outer boundary and is exposed to a normally applied load with constant intensity q. The plate material will be assumed to be homogeneous.

Deflection W of the plate under its own weight is described by the differential equation [5, 6]

$$D\Delta^2 W = q\,,$$

$$D = \frac{EH^3}{12(1-\nu^2)}\,, \quad \Delta = \frac{1}{r}\left[\frac{\mathrm{d}}{\mathrm{d}r}\left(r\,\frac{\mathrm{d}}{\mathrm{d}r}\right)\right],$$

where E is the Young's modulus, and H the plate thickness. In the case of hinge support, the deflection and the bending moment are zero at the outer boundary:

$$W(R) = M_r(R) = 0\,.$$

Whence follows the relationship

$$W(r) = \frac{qR^4}{64D}\left(\frac{r^4}{R^4} - 2\,\frac{3+\nu r^2}{1+\nu R^2} + \frac{5+\nu}{1+\nu}\right) + \frac{qH^2(R^2-r^2)}{20D(1-\nu^2)}\,,$$

and the deflection at the plate center (at $r = 0$) is given by

$$W_{\mathrm{c}} = \frac{qR^4}{64D}\,\frac{5+\nu}{1+\nu}\left[1 + \frac{16H^2}{5(1-\nu)(5+\nu)\,R^2}\right]. \tag{11}$$

Let us define the thickness H of such a mirror, for which the level of the optical surface distortions would be defined by the maximal deflection in the plate center under its own weight. For this purpose, instead of the bulk weight load, we will use a surface one with the intensity $q = \rho g H$ (ρ is the plate material density, and g the free-fall acceleration). By solving equation (11) with respect to H, we obtain

$$H = \sqrt{\frac{A}{W - AB}}\,,$$

where

$$A = \frac{3}{16}\,\frac{\rho g R^4(1-\nu)(5+\nu)}{E}\,, \quad B = \frac{16}{5}\,\frac{\nu}{(1-\nu)(5+\nu)\,R^2}\,.$$

Table 3 shows the values of the thickness H and the mass M of a monolithic mirror with a diameter of 1 m, which provides the above-mentioned deflection of no more than 1 μm for various materials. As one can see from the table, the reduction in the monolithic mirror mass can be achieved by utilizing materials with high specific stiffness and small specific weight, such as beryllium silicon and silicon carbide. An analysis of the dependence of W_{c} and mass M on thickness H demonstrates that the reduction in a mirror deflection under its own weight requires increasing its thickness and mass.

Table 3. Characteristics of a monolithic mirror no more than 1 m in diameter providing its deflection no more than 1 μm in size.

Material	ρ, g sm^{-2}	E, 10^{-5} MPa	ν	H, sm	M, kg
Copper	8.9	1.2	0.3	19	1300
Invar	8.0	1.5	0.3	16	1000
Beryllium	1.85	3.0	0.1	6	100
Molybdenum	10.2	3.3	0.3	12	950
Silicon	2.3	1.5	0.3	9	180
Silicon carbide	3.2	4.0	0.3	4	120

5. Large-sized mirrors from materials with cellular and porous structures

An efficient method for reducing the mass of large-sized mirrors is to employ a multilayered construction with the cellular or porous filling, consisting of bearing layers and the filler located between them.

In such a construction, the bearing layers almost fully resist the longitudinal loads (stretching, compression, and shift) in their planes and the transverse bending moments, which determines the bending stiffness of the whole construction [7]. The key to the mass reduction lies in minimizing the amount of material on the neutral surfaces, where it has small effect on decreasing the stiffness.

The ratio of the thickness to the characteristic size (diameter) for large-sized mirrors is $H/R \approx 0.2-0.3$, whereas the construction employed in aviation, space technology, and building has three layers with a relative thickness of less than 0.1. Therefore, the results of most studies related to the calculation of stress-strained states of three-layer plates in aircraft and building construction cannot be applied for designing weight-reduced large-sized mirrors. The main goal of the latter process is to obtain such a bending stiffness of the device that the deflections of the optical surface appearing under the load types mentioned above do not exceed the acceptable limit.

One can calculate and optimize the design of a large-sized mirror with a cellular or porous filling by assuming that the mirror consists of a reflecting plate, heat exchanger, upper bearing layer, filler, and lower bearing layer. It is very hard to rigorously solve such a problem, so in order to obtain clear expressions and analyzable calculation methods one needs to introduce various simplifying assumptions and hypotheses.

As in the case of monolithic construction, the introduced assumptions allow reducing the study of stress-strained states of multilayered stacks to the determination of the deflection and deformation in the region of the reference surface. The main difference between calculations for constructions with cellular or porous fillers and those for monolithic plates is in the accounting for the filler shear deformations. Therefore, one should find conditions under which the shear deformations inside the filler can be disregarded.

For a homogeneous loading of both bearing layers of the three-layer stack with mass forces q, the deflection of a three-layer plate which is freely supported along the boundary is given by [8]

$$W = \frac{qR^4}{EH^2\delta}\left\{ -\frac{1}{64}\left[\frac{5+\nu}{1+\nu} + \left(\frac{r}{R}\right)^4 - \frac{2(3+\nu)}{1+\nu}\left(\frac{r}{R}\right)^2\right] + \frac{E\delta H}{GR^2}\left[1-\left(\frac{r}{R}\right)^2\right]\right\},$$

where R is the radius, H the thickness of the whole device, δ the thickness of the bearing layers, E the elasticity modulus of the bearing layer material, and G the shear modulus of the filler.

In the center of the plate, the deflection takes the form

$$W = \frac{qR^4}{EH^2\delta}\left(\frac{5+\nu}{64(1+\nu)} + \frac{E\delta H}{GR^2}\right).$$

The second term in the parentheses accounts for the influence of shear strains. It is positive, so the appearance of shear deformations in the filler leads to an increase in the optical surface deflection under the action of mass forces. The relative error, which appears if the shear strain influence is ignored, becomes less than 15%, if the following inequality is fulfilled:

$$\frac{R^2}{H\delta}\frac{G}{E} \geqslant 100\,.$$

This inequality is nothing more than an applicability condition for the model of a multilayered rigid plate used for the calculation of weight deflections in large-sized mirrors.

Let us now assume that under the action of a homogeneously distributed luminous load the upper bearing layer heats by ΔT. We would also imply that its temperature has a linear spatial distribution. The maximal deflection of the mirror can then be expressed as

$$W = \frac{M_T R^2}{20E\delta H^2}\left(1 + 2\,\frac{E\delta^3}{GHR^2}\right).$$

Here, M_T is the temperature moment, and the second term in parentheses takes into account the influence of the shear rigidity of the cellular filler. The relative error for the definition of optical surface thermoelastic distortions using the model of a-layered rigid mirror would be less than 15% if the following inequality holds

$$\frac{HR^2G}{\delta^3E} \geqslant 10\,.$$

This means that we know the conditions under which one can use simplified models which do not take into account shear deformations inside the filler, and, particularly, the model of a multilayered plate with reduced characteristics. When calculating real constructions, the filler is replaced by some arbitrary material, which is homogeneous, orthotropic, or isotropic with reduced characteristics defined by the principle of equivalent work performed by the real and arbitrary filler. It is important here to obtain high specific flexural rigidity of the plate in order to reduce the distortion of the optical surface under its own weight and to resist thermal deflections caused by the luminous load.

Table 4. Results of calculations of deformations for large-sized mirrors 1 m in diameter.

Material	Mass, kg	Stabilization time	Deflection under own weight, μm	Thermal strains, μm
Beryllium	250	10 min	0.1	2.2
Silicon carbide	350	15 min	0.15	1.0
Invar	900	3 h	1.0	0.4
Molybdenum (cells)	200	1 s	0.2	2.1
Titanium (cells)	130	3 s	0.25	8.5
Invar (Cells)	230	5 s	0.8	0.7

As the thickness of the multilayered stack increases due to increasing the distance between the layers, the flexural rigidity of the construction increases proportionally to the thickness squared of the filler providing the joint operation of the bearing layers. The reduced elasticity modulus of the filler in the plane parallel to the optical surface is much smaller than that of the bearing layers, so the main type of filler deformation that causes optical surface deflection is the transverse shear. The smaller is the shear modulus of the filler, and the larger is the relative thickness, the larger are the shear strains.

Calculated results for deformations developed in large-sized mirrors 1 m in diameter fabricated from various materials are listed in Table 4. As one can see from the table, the application of cellular structures can significantly reduce the total mass of the mirror and its stabilization time, while maintaining the optical surface distortions at an acceptable level. Figure 3 shows an example of an invar cellular structure. Figure 4 depicts a large-sized mirror made of porous copper with a diameter of 1 m and thickness of 100 mm [9].

Good results should be expected when designing large-sized mirrors made of composite materials with a cellular structure. Methods for the fabrication of such materials are quite well developed. Of the most interest are carbon–silicon–silicon carbide composites. By connecting the cellular frame with monolithic plates of the same material, one can form a multilayered cellular stack with an efficient thermal stabilization system inside. Figure 5 demonstrates one of the types of cellular mirror templates made of a carbon–silicon–silicon carbide composite material.

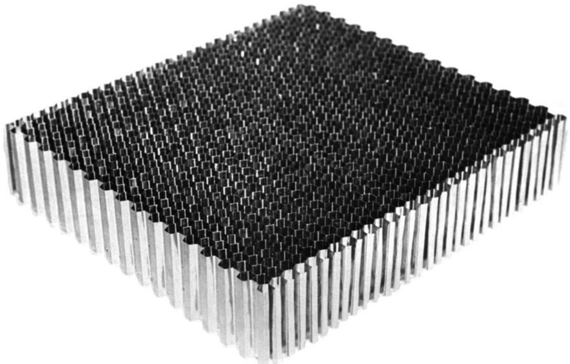

Figure. 3. Invar cellular structure.

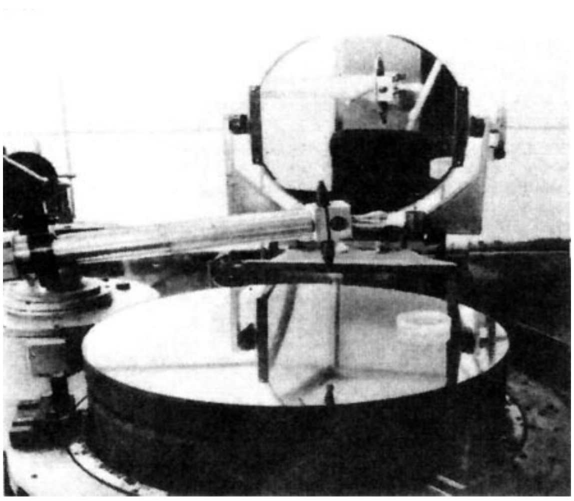

Figure. 4. Porous copper mirror 1 m in diameter

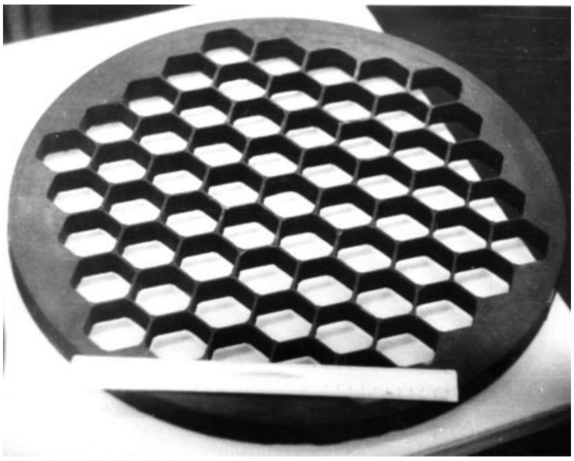

Figure. 5. Cellular structure made of a carbon–silicon–silicon carbide composite material.

6. Conclusion

The development of physical principles for the fabrication of large-sized laser mirrors is of great scientific and practical interest. This article suggests a calculation method for thermal deformations of laser mirrors under luminous load. We analyze the thermal stability dependence of cooled mirrors on the characteristics of the materials used. The results of investigations on the development of weight-reduced large-sized mirrors are shown for materials like invar, silicon carbide, and a carbon–silicon–silicon carbide composite.

References

1. Shmakov V A *Silovaya Optika* (Power Optics) (Moscow: Nauka, 2004)
2. Apollonov V V et al. *Sov. Tech. Phys. Lett.* **1** 240 (1975); *Pis'ma Zh. Tekh. Fiz.* **1** 522 (1975)
3. Apollonov V V et al. *Sov. J. Quantum Electron.* **11** 1344 (1981); *Kvantovaya Elektron.* **8** 2208 (1981)
4. Apollonov V V, Prokhorov A M, Shmakov V A *Quantum Electron.* **33** 655 (2003); *Kvantovaya Elektron.* **33** 655 (2003)
5. Love A E H *A Treatise on the Mathematical Theory of Elasticity* (Cambridge: Univ. Press, 1892, 1893); Translated into Russian: *Matematicheskaya Teoriya Uprugosti* (Moscow–Leningrad: ONTI, 1935)
6. Timoshenko S, Woinowsky-Krieger S *Theory of Plates and Shells* (New York: McGraw-Hill, 1959); Translated into Russian: *Plastinki i Obolochki* (Moscow: Nauka, 1963)
7. Kobelev V N, Kovarskii L M, Timofeev S I *Raschet Trekhsloinykh Konstruktsii* (Three-Layer Construction Calculations) (Moscow: Mashinostroenie, 1984)
8. Bryukker L E, Naumova M P "Simmetrichnyi izgib kruglykh trekhsloinykh plastin s legkim zapolnitelem" ("Symmetric bending of round three-layer plates with low-weight filler"), in *Raschety Elementov Aviatsionnykh Konstruktsii* (Calculations Elements of Aircraft Constructions) Issue 4 (Ed. R E Lamper) (Moscow: Mashinostroenie, 1965) p. 86
9. Alekseev V A et al. *Sov. Tech. Phys. Lett.* **11** 556 (1985); *Pis'ma Zh. Tekh. Fiz.* **11** 1350 (1985)